nature photonics

LETTERS

PUBLISHED ONLINE: 21 JUNE 2009 | DOI: 10.1038/NPHOTON.2009.99

Voltage-programmable liquid optical interface

C. V. Brown*, G. G. Wells, M. I. Newton and G. McHale

Recently, there has been intense interest in photonic devices based on microfluidics, including displays[1,2] and refractive tunable microlenses and optical beamsteerers[3–5] that work using the principle of electrowetting[6,7]. Here, we report a novel approach to optical devices in which static wrinkles are produced at the surface of a thin film of oil as a result of dielectrophoretic forces[8–10]. We have demonstrated this voltage-programmable surface wrinkling effect in periodic devices with pitch lengths of between 20 and 240 μm and with response times of less than 40 μs. By a careful choice of oils, it is possible to optimize either for high-amplitude sinusoidal wrinkles at micrometre-scale pitches or more complex non-sinusoidal profiles with higher Fourier components at longer pitches. This opens up the possibility of developing rapidly responsive voltage-programmable, polarization-insensitive transmission and reflection diffraction devices and arbitrary surface profile optical devices.

The device structure is shown in Fig. 1. The side view (Fig. 1a) shows the glass substrate coated with patterned gold/titanium conducting electrodes, on the top of which there is a thin solid dielectric layer (either photoresist or a dielectric stack), upon which is coated a thin layer of oil. The electrodes were arranged as an array of stripes parallel to the y-direction in the xy-plane. This geometry allowed every other electrode to be electrically connected as shown in the plan view in Fig. 1b.

Electrically induced wrinkling at the oil surface will be considered first for a device with an electrode pitch p of 80 μm. When a small volume (0.1 μl) of 1-decanol was initially dispensed onto the device it formed a spherical cap with a contact angle of 5°. Every other stripe in the electrode array was biased with an a.c. voltage of magnitude V_0 (r.m.s.) and the interdigitated stripes between them were earthed as shown in Fig. 1. This created a highly non-uniform, periodic electric field profile in the plane of the oil layer. A polarizable dielectric material in a region containing non-uniform electric fields experiences a force (known as a dielectrophoretic force) in the direction of the increase in magnitude of the electric field[8–10]. When the r.m.s. electrode voltage was greater than $V_0 = 20$ V the dielectrophoretic forces spread the oil into a thin film of uniform thickness $\bar{h} = 12$ μm, across the area covered by the electrodes.

Increasing the voltage between neighbouring electrodes gave rise to a periodic undulation at the surface of the oil. The period of the wrinkle was equal to the electrode pitch, 80 μm, and the peaks and troughs of the wrinkle lay parallel to the electrode fingers along the y-direction. This undulation arises because the highest electric field gradients occur in the gaps between the electrodes and so the dielectrophoretic forces in these regions cause the oil to collect there preferentially. The interdigitated electrode geometry is commonly used in biological particle manipulation[9,11] but dielectrophoretic actuation in fluids has previously been limited to nanodroplet formation and lab-on-a-chip applications[12].

The wrinkle at the oil–air interface and the associated periodic variation in the optical path for light travelling through the

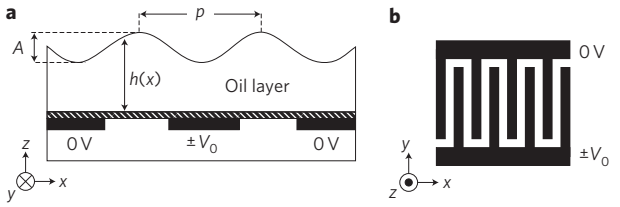

Figure 1 | Structure of the device. a, Side view. A thin layer of oil coats a dielectric layer (shown cross-hatched), which has been deposited onto a glass substrate containing an array of gold/titanium interdigitated striped electrodes (shown by the black electrodes). **b**, Plan view of the interdigitated electrode geometry.

film has been directly visualized here using a Mach–Zehnder interferometer[13]. The device was illuminated in transmission mode with He–Ne laser light at a wavelength of 633 nm. One of the mirrors of the interferometer was tilted to produce parallel intensity interference fringes localized at the position of the oil layer. The individual interference fringes were oriented parallel to the x-direction and a periodic change in the oil thickness $h(x)$ caused a directly proportionate periodic shift of the fringes in the y-direction. The interferograms shown as insets in Fig. 2 show the fringe patterns when voltages (20 kHz a.c.) of $V_0 = 80$ V (top left inset) and $V_0 = 160$ V (top right inset) were applied between adjacent in-plane electrodes.

Knowledge of the refractive index of the oil ($n_{oil} = 1.438$ for 1-decanol, ref. 14) allowed the peak-to-peak amplitude A of the wrinkle at the oil–water interface to be calculated directly from the interferometer fringe patterns. The results are shown as filled circles in Fig. 2, where the square of the r.m.s. amplitude of the applied voltage is plotted as the abcissae. The solid line shows the linear regression fit to the data: $A = (5.107 \times 10^{-5})\, V_0^2 + 0.118$, in micrometres.

Under an applied periodic potential the appearance of the wrinkle at the oil–air interface decreases the dielectric energy of the system, but this in turn causes an increase in the area of the oil–water interface. The interfacial surface tension provides a restorative force that resists the undulation deformation on the spread oil film. The observed dependence on the square of the voltage is reproduced by a simple calculation using the following approximations: (i) the wrinkle amplitude is small ($A \ll p$); (ii) the periodic potential profile due to the electrodes, $V(x, y)$, is described by a Fourier series expansion to second order only; and (iii) the potential profile is unperturbed by the presence of the oil–air interface. Equating and minimizing the sum of the electrostatic and surface tension energies with respect to the peak-to-peak amplitude A of the wrinkle yields equation (1):

$$A = \left[\frac{16\varepsilon_0}{3\gamma\pi^4}(\varepsilon_{oil} - \varepsilon_{air})\exp\left(-\frac{4\pi\bar{h}}{p}\right)\right]V_0^2 \qquad (1)$$

School of Science and Technology, Nottingham Trent University, Clifton Lane, Nottingham, NG11 8NS, UK. *e-mail: carl.brown@ntu.ac.uk

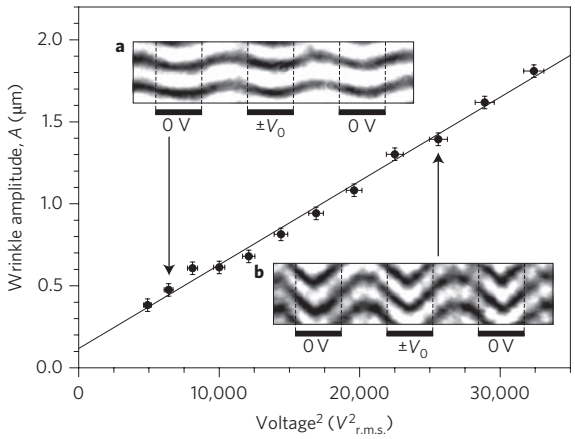

Figure 2 | Plot of the peak-to-peak amplitude *A* of the wrinkle at the oil–air interface and interferograms at different voltages. The insets present interferograms showing periodic displacements of tilt fringes at a wavelength of 633 nm (0.61 mW cm^{-2} at device) in a Mach–Zehnder interferometer. These fringe patterns were produced by a layer of 1-decanol oil coating a device with a dielectric stack of thickness 1.13 μm (see Supplementary information) with voltages (r.m.s. 20 kHz a.c.) of 80 V (top-left inset) and 160 V (bottom-right inset). The electrode (and wrinkle) pitch was 80 μm. The peak-to-peak amplitude *A* of the wrinkle at the oil–air interface was obtained from the interferometer fringe patterns and is plotted against the square of the a.c. voltage, V_0^2.

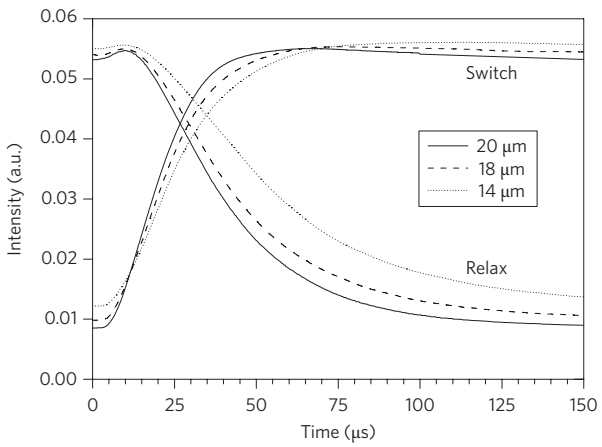

Figure 3 | Transient response of the intensity of the reflection mode first diffracted order as a function of time. Data were taken at a wavelength of 543 nm (0.08 W cm^{-2}) after a wrinkle of amplitude $A = 0.36$ μm at the surface of 1-decanol was turned on ('Switch') or off ('Relax') at time 0 μs. Measurements are shown for oil layers of three different thicknesses coating the same device as used in Fig. 2, for which the pitch was $p = 80$ μm.

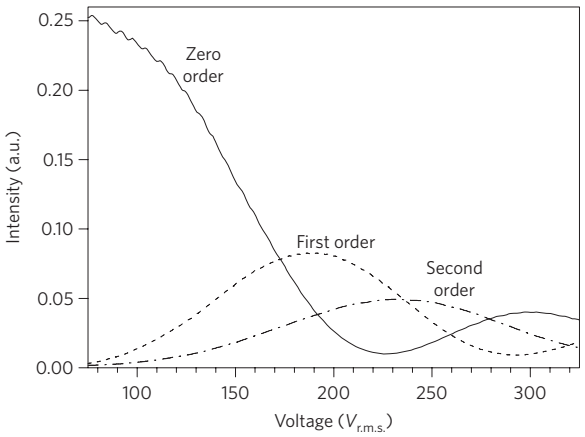

Figure 4 | Intensity of the zero-, first- and second-order peaks due to the diffraction of light at 543 nm. Intensities of the transmitted diffracted orders at 543 nm (0.08 W cm^{-2}) are shown for a film of 1-decanol with average thickness $\bar{h} = 3$ μm as a function of the magnitude of the voltage (20 kHz a.c.) applied between adjacent in-plane electrodes. The orders were observed at angles of 0° (zero), 1.56° (+1) and 3.11° (+2). For this device the dielectric layer was 2 μm thick and was fabricated from SU-8 photoresist (see Supplementary information), and the electrode pitch was $p = 20$ μm, which also corresponded to the wrinkle pitch.

This reproduces the intuitive result that, at a particular voltage, higher wrinkle amplitudes will result from using oil with a higher dielectric constant and lower surface tension. Substituting the values from the linear regression fit to the data in Fig. 2 and the values of $\varepsilon_{oil} = 8.1$ and $\gamma = 28.4$ mN m^{-1} (ref. 14) for the dielectric constant and surface tension of 1-decanol into equation (1) yields $\bar{h} = 5.5$ μm. This is the correct order of magnitude but lower than the average thickness of $\bar{h} = 12$ μm estimated from the fringe pattern at the edge of the spread film (see Supplementary information).

The switching speed was measured by monitoring the time-dependent intensity of the reflection mode first-order diffraction peak in response to a sudden change in the amplitude of the voltage V_0. The device was illuminated in reflection with laser light at a wavelength of 543 nm and the applied voltage (20 kHz a.c. square-wave) was discontinuously switched between a low value, $V_0 = 10$ V, and a high value every 5 ms. The low value was just sufficient to maintain the uniformity of the oil coating. The high value of the voltage was adjusted to achieve a peak in the intensity of the first diffracted order for each particular oil film thickness. For the three different thicknesses $\bar{h} = 20$, 18 and 14 μm, the r.m.s. amplitudes of the high voltages were $V_0 = 93$, 90 and 86 V, respectively. From simultaneous transmission measurements of the high-voltage fringe displacements on the Mach–Zehnder interferometer this was found to correspond to a wrinkle of amplitude $A = 0.36$ μm for all cases. Data are shown in Fig. 3 for the low to high voltage transition labelled 'Switch', and for the high to low voltage transition labelled 'Relax'. The times for the intensity to change from the value at 0 μs to 90% of the difference between the initial and asymptotic intensities were 35, 40, 49 μs (switching) and 79, 89, 108 μs (relaxing) for $\bar{h} = 20$, 18 and 14 μm, respectively.

An amplitude-programmable phase diffraction grating[15] has been demonstrated in transmission mode using wrinkles with a shorter pitch of $p = 20$ μm in a film of 1-decanol oil having an average thickness of $\bar{h} = 3$ μm. Figure 4 shows the intensities of the zero-, first- and second-order peaks due to the diffraction of light at 543 nm transmitted through the film with its periodic surface wrinkle as a function of the voltage V_0 (20 kHz a.c.) (see also Supplementary information).

The ratio of the peak intensity in the first order to the zero-order peak intensity at low voltage is 32.6%. This is close to the value of 33.8% that would be predicted by the Fraunhofer approximation for a 'thin sinusoidal phase grating'[16].

Still shorter pitches on the scale of micrometres or lower appear feasible, but there are technological challenges in creating a sufficiently thin film of oil. Still higher diffraction efficiencies may be possible by making the fluid surface (rather than the substrate) fully reflective[17,18]. It is also possible that the surface wrinkle could be produced at the interface between two density-matched liquids, for example, a high-refractive-index oil and water, in an encapsulated device that could be used in any orientation[3] (see Supplementary information).

Figure 5 shows oil film surface shapes that are more interesting than the simple sinusoidal profiles that have been discussed above. Each of

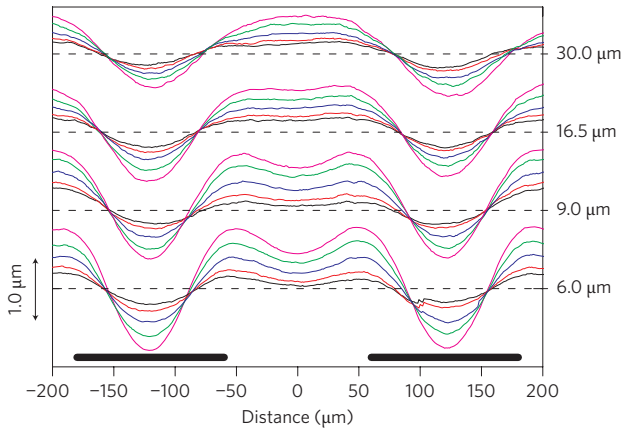

Figure 5 | Profiles at a hexadecane oil–air interface that have been created by the action of a non-uniform electric field profile. The profiles were measured using a Mach–Zehnder interferometer (633 nm and 0.61 mW cm^{-2} at the device). Oil films with four different thicknesses were used, $\bar{h}$ = 6.0, 9.0, 16.5 and 30.0 μm, as indicated by the dotted lines. At each different thickness the profiles obtained with different applied voltages are shown by solid lines of different colours: $V_{r.m.s.}$ = 275 V (black), 325 V (red), 400 V (blue), 475 V (green) and 550 V (magenta). For this device the dielectric layer was 2 μm thick and was fabricated from SU-8 photoresist (see Supplementary information), and the electrode pitch was p = 240 μm, which also corresponded to the wrinkle pitch. The positions of the electrodes are shown by the black lines at the bottom of the figure. The vertical scale is the same for each profile, but the profiles at different thicknesses have been displaced vertically for clarity.

the solid lines shows an individual surface profile that has been created for a particular voltage (represented using different colours) and for a particular average oil film thickness (shown by the horizontal dotted line on which it lies). By using oil with a lower dielectric constant (hexadecane, ε_{oil} = 2.05), combined with a longer electrode pitch (p = 240 μm), it has been possible to program non-sinusoidal profiles and so switch on other Fourier components with higher spatial frequencies. These higher Fourier components are most prominent at the lowest film thickness, $\bar{h}$ = 6.0 μm, where the surface of the oil film lies closer to the highly non-uniform fringing electric fields at the electrode edges.

In conclusion, we have presented a new and potentially versatile concept of using dielectrophoretic forces to create fluid-based optical switching devices. As an example photonic device application we have demonstrated a switchable phase diffraction grating where the intensity modulation of the undeviated zero order, as well as the diffracted orders, are intrinsically polarization insensitive; the zero- and first-order intensities can be fully modulated at speeds below 40 μs. The voltage-programmable optical effect uses a straightforward device structure and is static, reproducible and stable[19–21] when switched on. This combination of properties in a single device is significant compared with existing technologies based on, for example, birefringent liquid crystals[22,23], electro-optic or acousto-optic modulators[24,25], or deformable polymer layers[26]. Our further demonstration of more complex non-sinusoidal surface wrinkle profiles suggests the possibility of producing aperiodic or arbitrary surface profiles using independently addressable electrodes for application in two-dimensional spatial light modulator arrays.

Videos showing the modulation of the diffraction pattern in response to a slowly ramping voltage (i) in transmission mode using the 20-μm pitch, and (ii) in reflection mode using the 80-μm pitch are available as Supplementary Information. The Supplementary Information also provides additional experimental details and discussion of equation (1).

Received 22 March 2009; accepted 21 May 2009; published online 21 June 2009

References

1. Hayes, R. A. & Feenstra, B. J. Video-speed electronic paper based on electrowetting. *Nature* **425,** 383–385 (2003).
2. Heikenfeld, J. & Steckl, A. J. High-transmission electrowetting light valves. *Appl. Phys. Lett.* **86,** 151121 (2005).
3. Berge, B. & Peseux, J. Variable focal lens controlled by an external voltage: An application of electrowetting. *Euro. Phys. J. E* **3,** 159–163 (2000).
4. Kuiper, S. & Hendriks, B. H. W. Variable-focus liquid lens for miniature cameras. *Appl. Phys. Lett.* **85,** 1128–1130 (2004).
5. Smith, N. R., Abeysinghe, D. C., Haus, J. W. & Heikenfeld, J. Agile wide-angle beam steering with electrowetting microprisms. *Opt. Express* **14,** 6557–6563 (2006).
6. de Gennes, P. G. Wetting: statics and dynamics. *Rev. Mod. Phys.* **57,** 827–862 (1985).
7. Mugele, F. & Baret, J. C. Electrowetting: from basics to applications. *J. Phys. Condens. Matter* **17,** R705–R774 (2005).
8. Pellat, H. Mésure de la force agissant sur les diélectriques liquides non électrisés placés dans un champ électrique. *C. R. Acad. Sci. Paris* **119,** 691–694 (1895).
9. Pohl, H. A. *Dielectrophoresis: The Behaviour of Neutral Matter in Non-Uniform Electric Fields, Cambridge Monographs on Physics* (Cambridge Univ. Press, 1978).
10. Lorrain, P. & Corson, D. R. *Electromagnetic Fields and Waves* 2nd edn (W. H. Freeman, 1970).
11. Pethig, R. Using inhomogeneous a.c. electrical fields to separate and manipulate cells. *Crit. Rev. Biotech.* **16,** 331–348 (1996).
12. Jones, T. B., Gunjii, M., Washizu, M. & Feldman, M. J. Dielectrophoretic liquid actuation and nanodroplet formation. *J. Appl. Phys.* **89,** 1441–1448 (2001).
13. Born, M. & Wolf, E. *Principles of Optics* 7th edn (Cambridge Univ. Press, 2005).
14. *Knovel Critical Tables* 2nd edn (Knovel, 2003).
15. Hutley, M. C. *Diffraction Gratings* (Academic Press, 1982).
16. Goodman, J. W. *Introduction to Fourier Optics* 2nd edn (McGraw-Hill, 1996).
17. Hubert, H. & Girault, H. H. Electrowetting: shake, rattle and roll. *Nature Mater.* **5,** 851–852 (2006).
18. Bucaro, M. A., Kolodner, P. R., Taylor, J. A., Sidorenko, A., Aizenberg, J. & Krupenkin, T. N. Tunable liquid optics: electrowetting-controlled liquid mirrors based on self-assembled janus tiles. *Langmuir* **25,** 3876–3879 (2009).
19. Herminghaus, S. Dynamical instability of thin liquid films between conducting media. *Phys. Rev. Lett.* **83,** 2359–2361 (1999).
20. Schäffer, E., Thurn-Albrecht, T., Russell, T. P. & Steiner, U. Electrically induced structure formation and pattern transfer. *Nature* **403,** 874–877 (2000).
21. Staicu, A. & Mugele, F. Electrowetting-induced oil film entrapment and instability. *Phys. Rev. Lett.* **97,** 167801 (2006).
22. Komanduri, R. K., Chulwoo, O. & Escuti, M. J. Reflective liquid crystal polarization gratings with high efficiency and small pitch, in *Liquid Crystals XII* (ed. Khoo, Iam Choon) *Proc. SPIE*, **7050,** 70500J (2008).
23. De La Tocnaye, J. L. D. Engineering liquid crystals for optimal uses in optical communication systems. *Liq. Cryst.* **31,** 241–269 (2004).
24. Eldada, L. Optical communication components. *Rev. Sci. Instrum.* **75,** 575–593 (2004).
25. Mias, S. & Camon, H. A review of active optical devices: I. Amplitude modulation. *J. Micromech. Microeng.* **18,** 083001 (2008).
26. Bowden, N., Brittain, S., Evans, A. G., Hutchinson, J. W. & Whitesides, G. M. Spontaneous formation of ordered structures in thin films of metals supported on an elastomeric polymer. *Nature* **393,** 146–149 (1998).

Acknowledgements

The authors gratefully acknowledge J. Fyson at Kodak (European Research) Ltd and N. J. Shirtcliffe and C. L. Trabi at Nottingham Trent University for fruitful discussions. G.W. gratefully acknowledges The EPSRC/DTI COMIT Faraday Partnership and Kodak (European Research) Ltd for funding.

Author contributions

C.V.B., M.I.N. and G.M. conceived the concept and planning. C.V.B., G.G.W. and M.I.N. designed the experiment. C.V.B. and G.M. carried out theoretical work. C.V.B. wrote the paper and G.G.W. performed the experimental work and data analysis.

Additional information

Supplementary information accompanies this paper at www.nature.com/naturephotonics. Reprints and permission information is available online at http://npg.nature.com/reprintsandpermissions/. Correspondence and requests for materials should be addressed to C.V.B.